ACS Macro Letters

Letter

Cite This: ACS Macro Lett. 2019, 8, 1096−1101

pubs.acs.org/macroletters

Mechanisms of Ion Transport in Block Copolymeric Polymerized Ionic Liquids

Zidan Zhang,[†] Jakub Krajniak,[‡,§] Jordan R Keith,[†] and Venkat Ganesan*[,†]

[†]Department of Chemical Engineering, University of Texas at Austin, Austin, Texas 78712, United States

[‡]Department of Computer Science, Katholieke Universiteit Leuven, Leuven, Belgium

Supporting Information

ABSTRACT: We present the results of a multiscale simulation framework investigating the ion transport mechanisms in multicomponent polymerized ionic liquids. Three different classes of polymeric ionic liquid systems, namely, random copolymers, lamellae forming block copolymers, and homopolymers, are constructed at the coarse-grained scale, and their atomistic counterparts are derived by using a reverse mapping method. Using such a framework, we investigate the influence of morphology on ion transport properties of such polymerized ionic liquids. Our results for ion mobilities are in qualitative agreement with experimental observations. Further analysis of random copolymer and block copolymer systems reveal that the reduced ion mobilities in such systems arise from the influence of architecture and morphology on ion coordination and intramolecular hopping events.

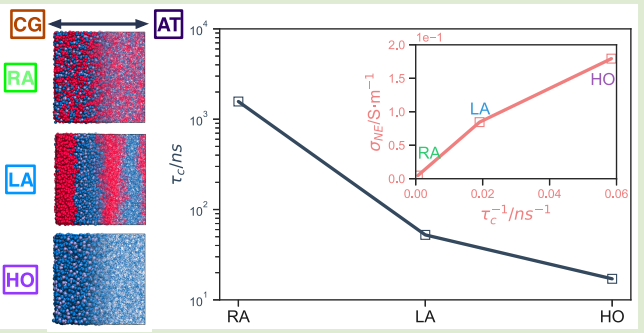

Self-assembled morphologies of block copolymers (BCP) containing polymerized ionic liquids (polyILs) are an emerging class of novel materials that are attracting interest in applications for lithium ion batteries.[1−3] It has been suggested that, by the appropriate choices of mechanically strong and conductive blocks and by tuning the morphology and domain sizes of the polyIL-BCPs, such materials could bypass the usual trade-offs between mechanical strength and conductivity.[4−10] Moreover, polyIL microdomains possess higher electrochemical stability compared to neutral block copolymers, which renders such systems attractive for lithium ion batteries.

Motivated by the above features, recent experimental studies have examined the influence of morphology on the ion transport properties of polyIL-BCPs. Elabd, Winey, and coworkers studied the electrochemical properties of multicomponent polyILs and observed that the ionic conductivities of the polyIL BCPs were approximately 2 orders of magnitude higher than their disordered polyIL random copolymer analogs at similar polyIL compositions. They attributed the higher conductivity of polyIL-BCPs to the microphase separation in BCPs.[6] In a different study, the same authors considered a strongly microphase-separated morphology (of a different polyIL-BCP) and showed an order of magnitude enhancement of conductivity arising from the enhanced microphase separation.[11]

While the above studies (and others) have highlighted the influence of microphase separation on ion transport in polyIL-BCPs, an understanding of the mechanisms underlying such observations is still lacking. In this context, we note a number of studies have considered the mechanisms of ion transport in microphase separated salt-doped neutral block copolymers.[12−15] In such materials, ion transport is assisted by the segmental motion of the polymers, and the influence of microphase separation has been rationalized through the combined influence of ion concentration profiles and the local segmental dynamics of the polymers.[16,17]

However, in comparison to the segmental dynamics assisted hopping mechanism in salt-doped polymer electrolytes, Mogurampelly and co-workers demonstrated that the ion transport mechanism in polyILs is governed by an association−dissociation process that they schematically termed as "ladder climbing", involving four polymeric cations from two different polymer chains.[18−20] As a consequence, the segmental dynamics of the polymers was shown to possess reduced significance in polyIL systems, and such results were used to rationalize the experimentally observed decoupling between ionic conductivities and glass transition temperatures in such materials.

Together, the above discussion points to the possibility that ion transport in polyIL-BCPs may involve physics different from those identified in salt-doped BCPs. Motivated by an objective to identify the transport mechanisms in multicomponent polyILs, in this letter, we report the results of a multiscale simulation approach which probed, at an atomistically resolved level, the structure and dynamics of three classes of polyIL systems: random copolymers (RA), diblock

Received: June 24, 2019
Accepted: August 7, 2019
Published: August 15, 2019

DOI: 10.1021/acsmacrolett.9b00478
ACS Macro Lett. 2019, 8, 1096−1101

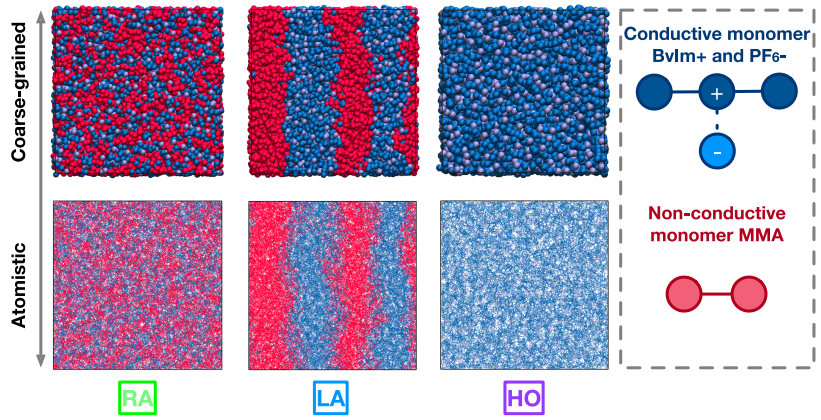

Figure 1. Morphologies under investigation: random copolymer (RA), lamellar block copolymer (LA), and homopolymer (HO). All three morphologies have the same number of ion pairs (1600). The detailed mapping scheme is shown in Figure S2, Supporting Information.

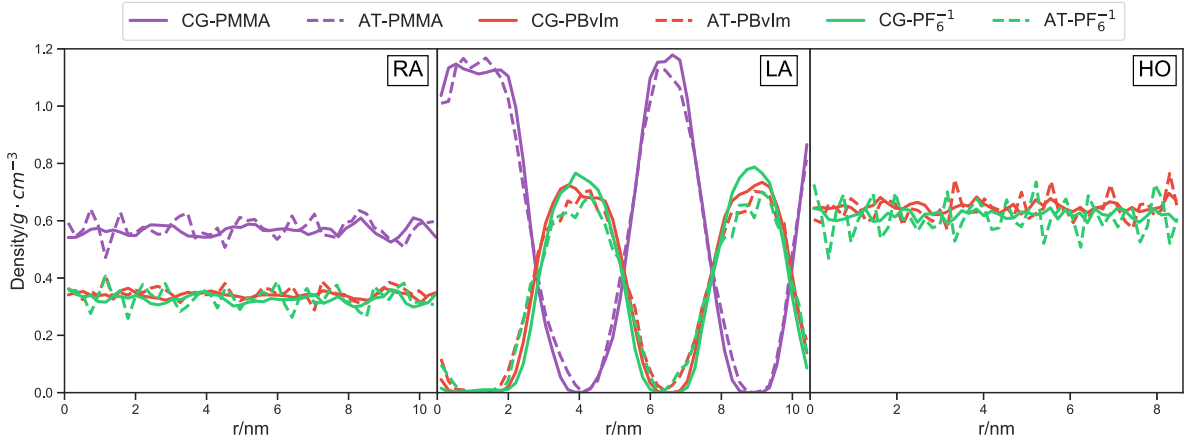

Figure 2. Comparison of the density profiles between coarse-grained and atomistic structures before and after reverse mapping.

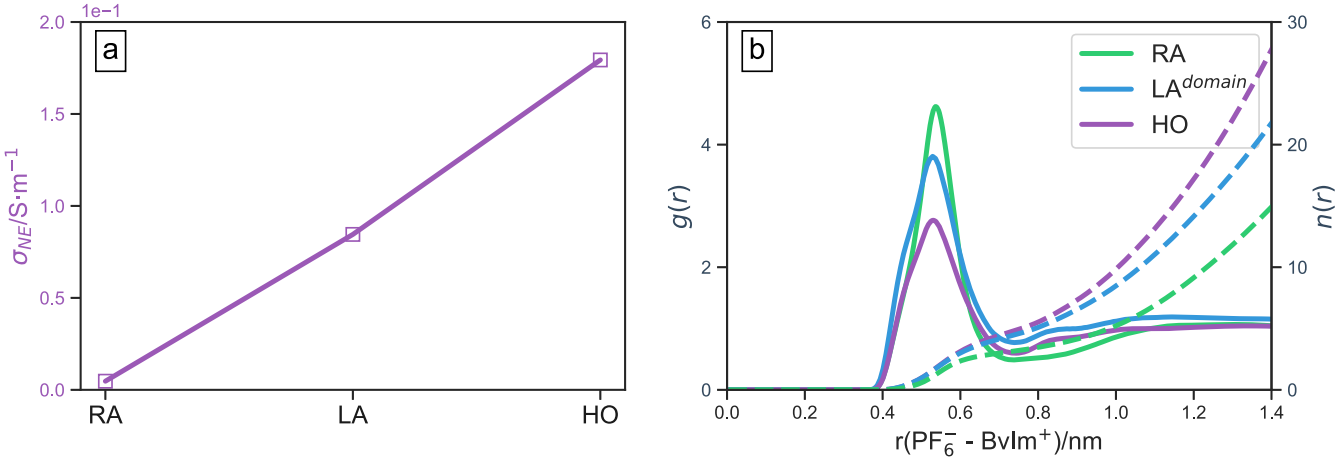

Figure 3. Ideal ionic conductivity (σ_{NE}): it has to be mentioned here that a scale factor of $\frac{3}{2}$ has been applied to the anion diffusion coefficient $D_{PF_6^-}$,[23] with the aim of making fair comparison between two-dimensional diffusion coefficient (LA) and three-dimensional diffusion coefficients (HO and RA) when calculating conductivity based on eq 1 (a); radial distribution functions $g(r)$ (solid lines) and the coordination number $n(r)$ (dash lines) for HO, LA, and RA: it also needs to be mentioned here that the calculated RDF for LA only considers the PBvIm-rich domain (b).

copolymers self-assembled in to lamellar phases (LA), and homopolymers (HO; cf. Figure 1).

Briefly, the multiscale simulation framework consists of three steps: The first step uses a simple "ideal" coarse-grained model to quickly converge the different systems to desired morphologies.[15] The second step bridges the ideal model and the real model with a coarse-grained (CG) model of higher chemical fidelity. Finally, the third step introduces chemical structural details via reverse mapping of the CG morphology.[21,22] In Supporting Information (section S1), we

DOI: 10.1021/acsmacrolett.9b00478
ACS Macro Lett. 2019, 8, 1096−1101

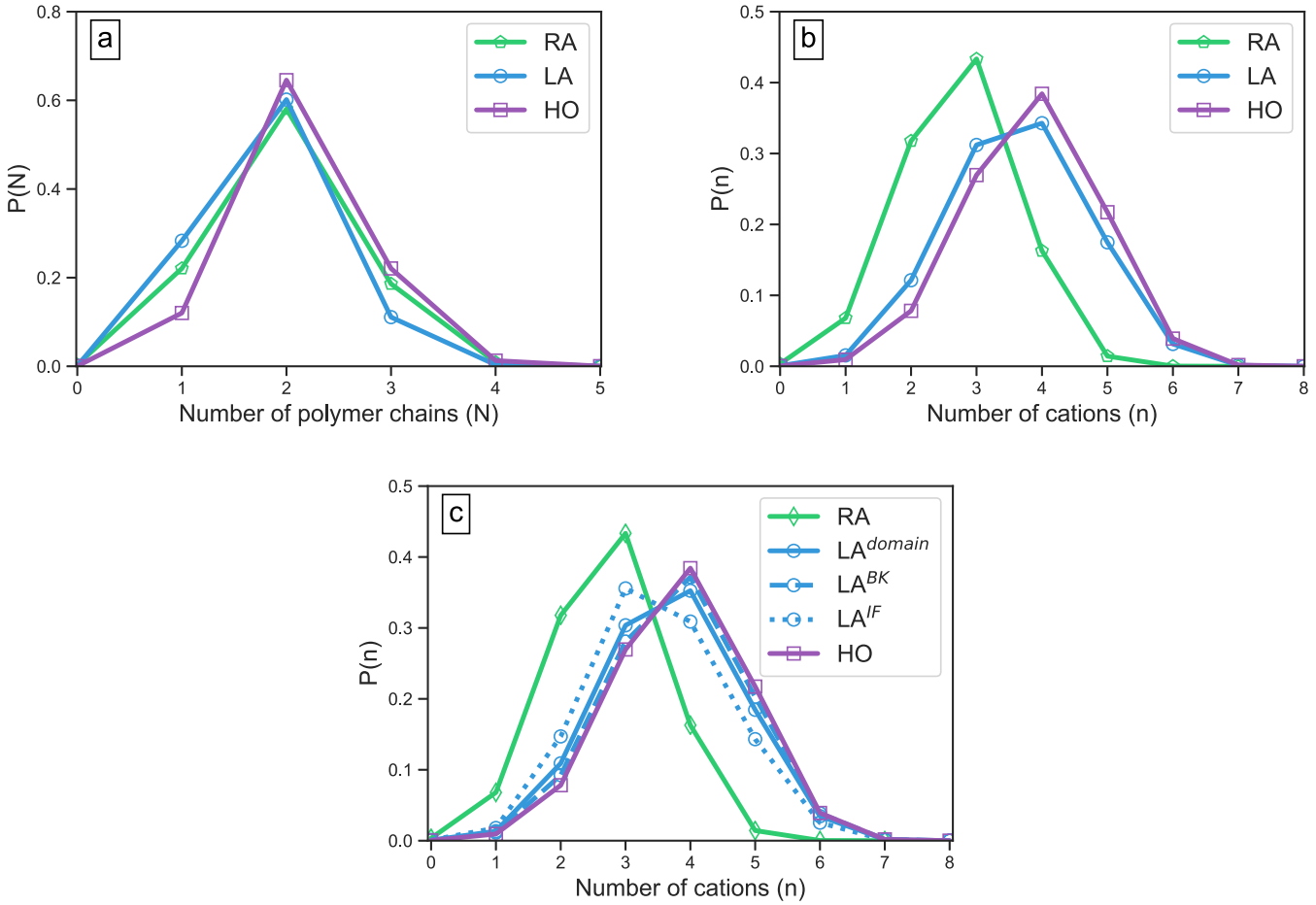

Figure 4. Probability that a given anion is associated with the number of polymer chains P(N) (a) and with number of cations P(n) (b), the corresponding association probability of the subgroups, namely, anion in the bulk region (LA^{BK}) and anion near the interface (LA^{IF}), is shown in (c).

provide some essential details of all three steps. In a separate publication, we plan to present a more detailed description of the multiscale simulation approach and its application to the simulation of other morphologies of polyIL-BCPs.

In Figure 2, we present results for the local density profile of the ions in the different morphologies derived through the coarse-graining and reverse mapping procedure. It can be seen that RA has the lowest local ion concentration (the total number of ion pairs were kept the same in the three different systems), a feature arising from the increased separation of cations in the polymer backbone by the nonconductive MMA monomers. In the case of LA, we observe that the anion concentration profile tracks the corresponding cation profiles and that, in the center of the lamella, the density of ions is close to the bulk conditions corresponding to that of the homopolymers.

To quantify the ion transport properties, we calculated the ideal, Nernst−Einstein ionic conductivities (σ_{NE}) as

$$\sigma_{NE} = \frac{N_{pair}}{V_\beta k_B T}\left(q^2_{PBvIm^+} D_{PBvIm^+} + q^2_{PF_6^-} D_{PF_6^-}\right) \quad (1)$$

where N_{pair} is the total number of ion pairs, V_β is the volume of the simulation box for β = {RA, LA, or HO}, k_B is the Boltzmann constant, q^+_{PBvIm} and $q^-_{PF_6}$ are the charges for cation and anion, D^+_{PBvIm} and $D^-_{PF_6}$ are the diffusion coefficients for cation and anion (the mean-squared displacements and their fits can be found in SI, section S2), respectively. In the time scale of our simulations, the polycations did not exhibit appreciable mobility to extract a diffusivity, and hence, we neglected the contribution of the mobility of polycations to σ_{NE}.

In Figure 3a we present the results for σ_{NE} as a function of morphology. We observe that σ_{NE} increases in the order RA to LA to HO, which is in qualitative agreement with observations from experiments.[6] More explicitly, an one-half reduction in σ_{NE} can be observed in transitioning from HO to LA, and an order of magnitude reduction in σ_{NE} in transitioning from LA compared to RA.

To rationalize the above observations, we recall that our previous work[18,19] demonstrated that anion transport in polyILs (HO) involves a process of hopping through a series of association−dissociation events involving associations with four cations from two different polymer chains. In such a context, the mobilities of the anions were demonstrated to be directly related to the time scale of such association−dissociation events. Further, the time scale for such hopping processes were shown to be correlated to the strength of interactions between the anions and the cations.[24]

To identify the mechanisms underlying the results in Figure 3a, we probed the influence of morphology and polymer sequence on the anion−cation interactions by calculating the radial distribution functions $g(r)$ (RDF, the method of the calculation of domain specific RDF can be found in SI, section

DOI: 10.1021/acsmacrolett.9b00478
ACS Macro Lett. 2019, 8, 1096−1101

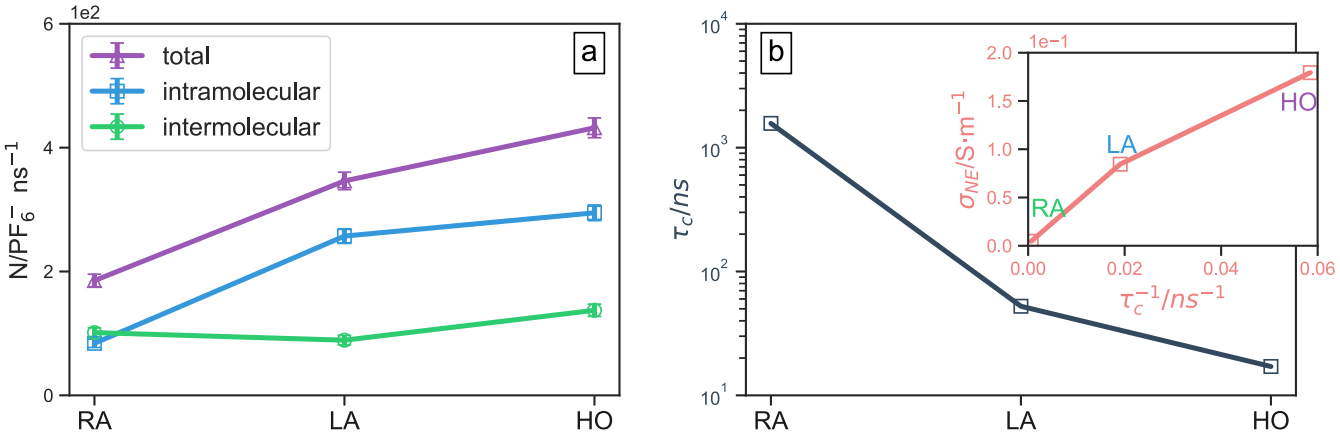

Figure 5. Average hopping events of a given PF_6^- in unit time period (a) and the ion-association relaxation time τ_c (b); inset to (b) displays the results for conductivity as a function of inverse τ_c.

S3) as well as the coordination number $n(r)$, and the results are displayed in Figure 3b. It can be seen there that the peak in the RDFs follow the order RA > LA > HO. Such trends can broadly be understood as a consequence of the local environment driving the interactions between the cations and anions. Indeed, in the case of RA, the local environment of the polycations is punctuated by the presence of nonconductive MMA monomers. Hence, the usually delocalized interactions between the anions and the cations are strengthened due to the lower concentration of polycations. In a similar manner, the interfacial region of the LA (cf. Figure 2) represents a mixture of the polycations and MMA monomers and is, hence, expected to lead to stronger anion−cation interactions, thereby influencing the domain-averaged RDF.

While the above results for $g(r)$ and $n(r)$ hints, at a simplistic level, to possible differences in cation−anion interactions in LA, RA, and HO systems, it does not address the influence, if any, of the morphology on the coordination characteristics and the mechanism of ion transport in multicomponent polyILs. To provide insights into such issues, we probed the cation−anion coordination characteristics and ion transport mechanisms in the three classes of polyILs. In Figure 4 we display $P(N)$ and $P(n)$, respectively, quantifying the probability of association of an anion (PF_6^-) with N polymer chains and n cations (deduced based on ions located in the first coordination shell, the cutoff distance is 0.65 nm, cf. SI section S4). Figure 4a identifies that in all three systems (HO, LA and RA), an anion exhibits an association state with maximal probability at two polymer chains. Such a result is in agreement with the results of our previous studies for HO systems.[18,19,25] In contrast, Figure 4b highlights distinct differences in *ionic* association behavior among the three systems. Specifically, for HO systems, our results are consistent with our earlier studies and demonstrate a peak at $n = 4$. In contrast, the $P(n)$ distribution for RA has a main peak located at $n = 3$. For LA, we observe a broad distribution with comparable probabilities for $n = 3$ and $n = 4$. To understand the results for LA, in Figure 4(c) we display $P(n)$ specifically for the IF (interface) and BK (bulk) zones in PBvIm-rich domain of LA (cf. SI section S5 for a description of the manner in these zones were identified) and compare with the distributions noted for RA and HO. It can be seen that the distribution for LA^{IF} has the same maximum peak (at $n = 3$) as that of RA, whereas the results for LA^{BK} aligns closely with that of HO. Such results suggest that the $P(n)$ noted for LA (Figure 4b) arises from a combination of (i) the frustrated coordination of anions near the interface of LA, which resembles the association characteristics in RA, and (ii) the normal coordination of anions in the bulk region of LA, which resembles the association features of HO.

The above results demonstrate that the morphology of self-assembly (LA) and chain architecture (RA) frustrates cation−anion coordination characteristics in polyIL systems. What is the influence of such modified coordination characteristics on ion transport? To address this question, we probed the modes of ion transport when they are associated with the polymer chains and classified them into two categories (Figure 5a): (i) intramolecular and (ii) intermolecular association events (the determination of these hopping events are described in SI section S6). It is observed that, while the number of intermolecular association events are comparable for three systems, the number of intramolecular hopping events exhibit very different characteristics. Explicitly, in agreement with our earlier results,[18] it can be seen that the intramolecular hopping events dominate the ion transport mechanism in HO. In contrast, for RA, the number to the intramolecular events are seen to be very few and comparable to the intermolecular hopping events. In comparing LA and HO, we observe a slightly lower extent of intramolecular hopping events in the LA, a trend that can be rationalized by again viewing the features in LA as a combination of the interfacial characteristics that resemble RA systems and the bulk characteristics that resemble HO systems.

Finally, to demonstrate the influence of the above coordination distributions and hopping characteristics on the dynamics of the anions, in Figure 5b, we display the ion-association relaxation time τ_c as a function of morphology (the calculation of τ_c as well as the average lifetime of ion-association pair, τ_s, can be found in SI, section S7). It can be seen that τ_c decreases in the order RA to LA to HO. More explicitly, τ_c for HO is three times faster than that for LA, and an order of magnitude enlargement in τ_c in transitioning from LA compared to RA. Such trends are in quantitative agreement to that of σ_{NE} (a result shown quantitatively in the inset of Figure 5b).

The results in Figures 3b−5 suggest a novel picture of the influence of chain architecture, morphology on ion transport in polyIL-BCPs. Specifically, the results of Figures 3b and 4 demonstrate that both RA and the interfacial zones of the BCP are characterized by stronger and frustrated anion−cation

DOI: 10.1021/acsmacrolett.9b00478
ACS Macro Lett. 2019, 8, 1096−1101

interactions relative to a HO system. The disordered RA system can be qualitatively pictured as one that contains a significant extent of interfacial zones distributed throughout the system and, hence, exhibits a much stronger (and more frustrated) anion−cation coordination characteristic compared to LA and HO. The presence of MMA monomers, either arising as a consequence of architecture (RA) or as a result of the interfacial region (LA), is seen to impact the cation−anion coordinations (Figure 4b) and, thereby, the mechanism of ion transport (Figure 5). Specifically, the number of intramolecular hopping events in RA and LA is reduced relative to the HO systems. As a consequence, the anion mobilities (which are proportional to the total number of hopping events) becomes (i) significantly reduced for RA and (ii) reduced (but to a lesser extent than RA) in LA. Correspondingly, the ion-association relaxation times become increased, leading to lower ion mobilities. We propose that such mechanisms underlie the conductivity results depicted in Figure 3a.

In summary, the results presented in this letter demonstrate novel features accompanying ion transport in multicomponent polyIL systems. The ion mobilities and the ideal conductivities were found to follow the order HO > LA > RA. Such results were rationalized at a simplistic level by invoking the strength of cation−anion coordinations, which were shown to be influenced by the presence of the nonconducting monomers. A more detailed analysis of the coordination and hopping mechanisms revealed that the interfacial zone of the LA (and the bulk regions of RA) was characterized by frustrated coordination behavior, which led to reduced intramolecular hopping and lower anion mobilities. Such results suggest that microphase separation influences ion transport in polyIL-BCPs through mechanisms that are significantly different from those identified for salt-doped (neutral) polymer systems.[12−15]

■ ASSOCIATED CONTENT

Supporting Information

The Supporting Information is available free of charge on the ACS Publications website at DOI: 10.1021/acsmacrolett.9b00478.

Section S1, the simulation details; Section S2, the fitting of diffusion coefficients for three morphologies; Section S3, the methodology of calculating domain specific RDF; Section S4, the definition for the first coordinate shell; Section S5, the calculation of interfacial area and width; Section S6, the definitions of intra/intermolecular hopping events; Section S7, the calculation of relaxation time scales (PDF)

■ AUTHOR INFORMATION

Corresponding Author

*E-mail: venkat@che.utexas.edu.

ORCID

Zidan Zhang: 0000-0002-6909-8742
Jakub Krajniak: 0000-0001-9372-6975
Jordan R Keith: 0000-0003-2639-3087
Venkat Ganesan: 0000-0003-3899-5843

Present Address

[§]Independent researcher, os. Kosmonautow 13/56, 61-631 Poznan, Poland.

Notes

The authors declare no competing financial interest.

■ ACKNOWLEDGMENTS

The authors work on the topic of ion transport in polymer electrolytes have been generously supported by grants from Robert A. Welch Foundation (Grant F1599) and the National Science Foundation (CBET-17069698 and DMR-1721512). The development of the multiscale simulation methodology was supported as part of the Center for Materials for Water and Energy Systems, an Energy Frontier Research Center funded by the U.S. Department of Energy, Office of Science, Basic Energy Sciences under Award #DE-SC0019272. The authors acknowledge the Texas Advanced Computing Center (TACC) for the generous allocation of computing resources.

■ REFERENCES

(1) Knychała, P.; Dziecielski, M.; Banaszak, M.; Balsara, N. P. Phase Behavior of Ionic Block Copolymers Studied by a Minimal Lattice Model with Short-Range Interactions. *Macromolecules* **2013**, *46*, 5724−5730.

(2) Wołoszczuk, S.; Banaszak, M.; Knychała, P.; Radosz, M. Monte Carlo Phase Diagram of Symmetric Diblock Copolymer in Selective Solvent. *Macromolecules* **2008**, *41*, 5945−5951.

(3) Knychała, P.; Banaszak, M.; Park, M. J.; Balsara, N. P. Microphase Separation in Sulfonated Block Copolymers Studied by Monte Carlo Simulations. *Macromolecules* **2009**, *42*, 8925−8932.

(4) Ganesan, V. Ion transport in polymeric ionic liquids: recent developments and open questions. *Molecular Systems Design & Engineering* **2019**, *4*, 280−293.

(5) Weber, R. L.; Ye, Y.; Schmitt, A. L.; Banik, S. M.; Elabd, Y. A.; Mahanthappa, M. K. Effect of Nanoscale Morphology on the Conductivity of Polymerized Ionic Liquid Block Copolymers. *Macromolecules* **2011**, *44*, 5727−5735.

(6) Ye, Y.; Choi, J.-H.; Winey, K. I.; Elabd, Y. A. Polymerized Ionic Liquid Block and Random Copolymers: Effect of Weak Microphase Separation on Ion Transport. *Macromolecules* **2012**, *45*, 7027−7035.

(7) Bouchet, R.; Maria, S.; Meziane, R.; Aboulaich, A.; Lienafa, L.; Bonnet, J.-P.; Phan, T. N. T.; Bertin, D.; Gigmes, D.; Devaux, D.; Denoyel, R.; Armand, M. Single-ion BAB triblock copolymers as highly efficient electrolytes for lithium-metal batteries. *Nat. Mater.* **2013**, *12*, 452.

(8) Sanoja, G. E.; Popere, B. C.; Beckingham, B. S.; Evans, C. M.; Lynd, N. A.; Segalman, R. A. Structure−Conductivity Relationships of Block Copolymer Membranes Based on Hydrated Protic Polymerized Ionic Liquids: Effect of Domain Spacing. *Macromolecules* **2016**, *49*, 2216−2223.

(9) Harris, M. A.; Heres, M. F.; Coote, J.; Wenda, A.; Strehmel, V.; Stein, G. E.; Sangoro, J. Ion Transport and Interfacial Dynamics in Disordered Block Copolymers of Ammonium-Based Polymerized Ionic Liquids. *Macromolecules* **2018**, *51*, 3477−3486.

(10) Mapesa, E. U.; Chen, M.; Heres, M. F.; Harris, M. A.; Kinsey, T.; Wang, Y.; Long, T. E.; Lokitz, B. S.; Sangoro, J. R. Charge Transport in Imidazolium-Based Homo- and Triblock Poly(ionic liquid)s. *Macromolecules* **2019**, *52*, 620−628.

(11) Choi, J.-H.; Ye, Y.; Elabd, Y. A.; Winey, K. I. Network Structure and Strong Microphase Separation for High Ion Conductivity in Polymerized Ionic Liquid Block Copolymers. *Macromolecules* **2013**, *46*, 5290−5300.

(12) Ozcam, A. E.; Petzetakis, N.; Silverman, S.; Jha, A. K.; Balsara, N. P. Relationship between Segregation Strength and Permeability of Ethanol/Water Mixtures through Block Copolymer Membranes. *Macromolecules* **2013**, *46*, 9652−9658.

(13) Ganesan, V.; Pyramitsyn, V.; Bertoni, C.; Shah, M. Mechanisms Underlying Ion Transport in Lamellar Block Copolymer Membranes. *ACS Macro Lett.* **2012**, *1*, 513−518.

(14) Seo, Y.; Brown, J. R.; Hall, L. M. Diffusion of Selective Penetrants in Interfacially Modified Block Copolymers from Molecular Dynamics Simulations. *ACS Macro Lett.* **2017**, *6*, 375−380.

DOI: 10.1021/acsmacrolett.9b00478
ACS Macro Lett. 2019, 8, 1096−1101

(15) Alshammasi, M. S.; Escobedo, F. A. Correlation between Ionic Mobility and Microstructure in Block Copolymers. A Coarse-Grained Modeling Study. *Macromolecules* **2018**, *51*, 9213−9221.
(16) Sethuraman, V.; Mogurampelly, S.; Ganesan, V. Multiscale Simulations of Lamellar PS-PEO Block Copolymers Doped with LiPF6 Ions. *Macromolecules* **2017**, *50*, 4542−4554.
(17) Sethuraman, V.; Mogurampelly, S.; Ganesan, V. Ion transport mechanisms in lamellar phases of salt-doped PS−PEO block copolymer electrolytes. *Soft Matter* **2017**, *13*, 7793−7803.
(18) Mogurampelly, S.; Keith, J. R.; Ganesan, V. Mechanisms Underlying Ion Transport in Polymerized Ionic Liquids. *J. Am. Chem. Soc.* **2017**, *139*, 9511−9514.
(19) Keith, J. R.; Mogurampelly, S.; Aldukhi, F.; Wheatle, B. K.; Ganesan, V. Influence of molecular weight on ion-transport properties of polymeric ionic liquids. *Phys. Chem. Chem. Phys.* **2017**, *19*, 29134−29145.
(20) Keith, J. R.; Mogurampelly, S.; Wheatle, B. K.; Ganesan, V. Influence of side chain linker length on ion-transport properties of polymeric ionic liquids. *J. Polym. Sci., Part B: Polym. Phys.* **2017**, *55*, 1718−1723.
(21) Krajniak, J.; Zhang, Z.; Pandiyan, S.; Nies, E.; Samaey, G. Reverse mapping method for complex polymer systems. *J. Comput. Chem.* **2018**, *39*, 648−664.
(22) Zhang, Z.; Krajniak, J.; Samaey, G.; Nies, E. A Parallel Multiscale Simulation Framework for Complex Polymerization: AB2-Type Monomer Hyperbranched Polymerization as an Example. *Advanced Theory and Simulations* **2019**, *2*, 1800102.
(23) Shen, K.-H.; Brown, J. R.; Hall, L. M. Diffusion in Lamellae, Cylinders, and Double Gyroid Block Copolymer Nanostructures. *ACS Macro Lett.* **2018**, *7*, 1092−1098.
(24) Keith, J. R.; Rebello, N. J.; Cowen, B. J.; Ganesan, V. Influence of Counterion Structure on Conductivity of Polymerized Ionic Liquids. *ACS Macro Lett.* **2019**, *8*, 387−392.
(25) Mogurampelly, S.; Ganesan, V. Ion Transport in Polymerized Ionic Liquid−Ionic Liquid Blends. *Macromolecules* **2018**, *51*, 9471−9483.

DOI: 10.1021/acsmacrolett.9b00478
ACS Macro Lett. 2019, 8, 1096−1101